International Journal on
"Technical and Physical Problems of Engineering"
(IJTPE)
Published by International Organization of IOTPE

ISSN 2077-3528
IJTPE Journal
www.iotpe.com
ijtpe@iotpe.com

September 2023 | Issue 56 | Volume 15 | Number 3 | Pages 68-76

AN ASYMMETRIC FUZZY LOGIC CONTROLLER BASED MPPT ALGORITHM FOR PV SYSTEM

S.K.W. Aldoori M.E. Yigit M. Ari

Electrical and Electronics Engineering Department, Cankiri Karatekin University, Cankiri, Turkey
kh.sarmad3@gmail.com, eyigit@karatekin.edu.tr, mari@karatekin.edu.tr

Abstract- When combined with an optimized control algorithm, such as the maximum-power-point-tracking (MPPT) method, renewable solar energy is a very efficient source of energy. However, the MPPT algorithm is a very cost-effective algorithm that ensures the least amount of energy loss in PV solar modules. In this paper, various controllers will be implemented and compared in order to maintain a highly efficient and robust controller-based MPPT algorithm, including the PI controller, the fuzzy-logic-controller (FLC), and the ANFIS controller. In addition, an effective DC-DC boost converter has been designed and integrated as well. The FLC based MPPT method has provided a maximum power of 106.1 watts, while the adaptive-neuro-fuzzy-inference-system (ANFIS) has allowed the PV solar system to extract its full energy.

Keywords: Asymmetric, MPPT, Fuzzy Logic, DC-DC Boost Converter, ANFIS, PV Solar.

1. INTRODUCTION

Solar energy is the most important source of renewable energy due to the end of fossil crops and environmental pollution [1]. Solar energy is considered among source of power the most significant renewable energy because it is a cost-free, endless, and environmentally friendly source, whether in stand-alone or grid-connected configurations. However, two major issues with photovoltaic (PV) systems are that the power conversion efficiency is significantly low and the continuous changes in electric power produced by solar modules follow the weather's conditions. So, the nonlinear behavior of PV output in terms of changes in temperature and solar irradiation means that the MPPT algorithm must be used to get the most energy out of PV solar modules [2].

The development in the semiconductor field provides an efficient technique including perturbation-and-observation (P&O), constant voltage (CV), incremental conduction (INC), fuzzy-logic-control (FLC), and artificial neural networks (ANN) [3]. The most accurate MPPT techniques are those based on ANN and ANC, although their design and implementation are complicated. Even though the most extensively used technique in commercial applications is the P&O technique, where the accuracy is moderate, the voltage/current feedback (VF/CF) is simpler in that it compares the module voltage or current with the pre-calculated values or the reference ones [4]. Moreover, a DC-DC boost-converter is built to ensure a fast and accurate MPPT algorithm to get the maximum energy from a PV solar system and to analyze the maximum energy delivery mechanism for a solar power system and its implementation for comprehensive system design.

2. LITERATURE REVIEW

Comparing different MPPT methods by using the MATLAB tool Simulink has been achieved, assuming radiation is uniformly scattered over the PV array [5, 6]. The Maximum Power Point of a solar cell is sought to be reached by various algorithms, to increase the efficiency of the solar panel. The reach of the MPP, as well as the complexity and need of measurement sensors are analyzed [7]. The mathematical model of each component is considered in the implementation of the PV system. Attention has focused on the grid-connected photovoltaic system generated by the primary single-ended DC/DC connection (SPEIC) between the grid and the solar panel [5, 8]. Ten different MPPT techniques are compared here. Solar isolation of twelve different types is considered, and the energy that is supplied by a complete PV system is calculated. It is concluded that the IC and P&O methods are the most effective MPPT methods among all the analyzed techniques [5]. Under changing conditions in climate, such as temperature and irradiance, successful implementation of perturb, observe, and fuzzy logic is achieved [6]. A DC-DC boost-converter model using FLC and the traditional MPPT method for P&O controllers was created in the MATLAB Simulink environment, and Simulink results were compared. The boost transformer is connected to increase the voltage of the PV module. The results referred to show that the performance of the fuzzy logic controller is rapid, accurate, and better than P&O under varying atmospheric conditions [6]. However, SPEIC DC-DC converters work better with no ripples or oscillations at PV module output voltage. Fuzzy logic controllers are used to maximize power under fluctuating temperatures and irradiation. According to this module, at a 1000 PV system, output power increases while cell temperature decreases [8].

Methods including the incremental conductance method (IncCond), constant voltage and turmoil monitoring method, and control method (P&O) were compared [7]. Investigation of the proposed system has been done via simulation and efficiency evaluation experiments of the methods. An analysis of the transient and steady-state characteristics of the control algorithm was conducted, and its efficiency was measured. Finally, the incremental conductance method and constant voltage control methods are combined, and a novel control algorithm is proposed in an attempt to enhance the efficiency of a (3 kW) photovoltaic power production system in various insolation terms. Under rapidly changing solar insolation conditions, the IncCond and P&O MPPT approaches have failed to follow the maximum power point. Because of the implementation of a modified constant voltage method, the two mode MPPT control method suggested in this paper performs excellently [7].

The study in [8] described that the P&O technique efficiency is low, unlike other P&O techniques, and that the reason for its low efficiency is a lack of speed while tracking MPP. The great efficiency of the ICb method does not justify the cost of using more than one sensor compared to the ICa method. IC techniques have nearly equal efficacy. Good results are produced by the TP temperature technique, but inconveniences are produced by variations in certain parameters that create errors in the evaluation of optimal voltage regarding its impact on the measured temperature due to a phenomenon unrelated to solar insulation. More research on the cost comparison of these techniques, particularly under shadow conditions, is required [9].

MPPT-based FLC has been implemented in the PV system [10, 11]. The MPPT-based hill climbing optimization technique is used to improve solar PV performance [11]. The major advantage of fuzzy logic is its efficiency and robust behavior in the face of changing radiation levels. A buck-boosted DC-DC regulator is used and implemented. Under conditions of changing solar irradiation, the output of the PV solar system can be controlled at its maximum value using an MPPT-based FLC. After installing an MPPT system during changing solar irradiation conditions, the average output voltage increased by 17%, from 11.6 V to 13.94 V. Power output increased by 28%, from 35.13 W to 48.9 W, after MPPT installation under changed solar irradiation conditions. Under changing temperature conditions, MPPT can keep the PV output voltage modules at the maximum required value of 12 V [11]. To achieve inversion, a PV system controlled by a single-phase bidirectional PMW converter and DC-DC converter is implemented [12]. While the MPPT algorithm is proposed and built on an ANN with FLC to enhance the system's performance [13],

In [14] created an MPPT-based Arduino microcontroller. The proposed system has low power consumption, low cost, and high-power efficiency. It allows for customized and easier system modifications and also facilitates data storage, remote monitoring, continuous displaying of system status, and external device charging. The experiment results with the 30 W prototype system are presented and validated. It is concluded that the average charge controller efficiency is 91.45%, satisfying the regulations of the technical standard committee (TSC) of the Infrastructure Development Company Limited (IDCOL) [14].

3. MODELLING OF A PHOTOVOLTAIC MODULE

3.1. PV Cell Characteristics

A PV panel has a negative electric field on the front side and a positive one on the back side, which is typical of silicon semiconducting resources. Solar cells, wires, shields, and supports make up a photovoltaic PV generator. Solar photons collide with a solar cell, breaking atomic bonds and releasing electrons. This "loosening" creates electron-hole pairs, which positive and negative electrical conductors connect to. Moving electrons generate an I_{ph}, which represents the electric current in a circuit. Solar cells operate like diodes in the dark. It's a p-n junction that blocks voltage and current. Connecting the cell to a high-voltage external source generates a ID current. Figure 1 shows that a solar cell's electrical activity commonly resembles a single diode [15]. Figure 1 shown the single PV solar cell equivalent circuit.

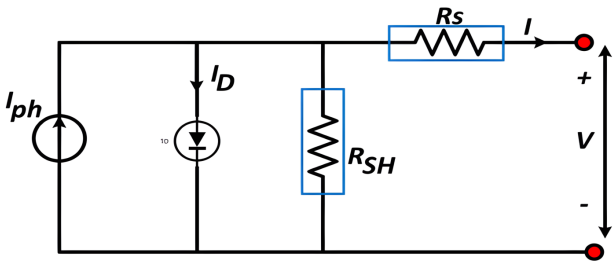

Figure 1. Single PV solar cell equivalent circuit [14]

The equivalent model comprises a current source I_{ph}, series resistance R_S, and a diode that simulates cell resistance. Figure 2 shows the diode's outside and interior shunt resistances related to the PV solar cell equivalent circuit. The resultant current can be calculated as follows [14]:

$$I = I_{ph} - I_D \tag{1}$$

$$I = I_{ph} - I_s\left(e^{\frac{q(V+I.R_s)}{K.T_{ref}}} - 1\right) - \frac{V + I.R_s}{R_{SH}} \tag{2}$$

where, I_{ph} is the produced current, q is the charge of the electron, K is the Boltzmann's constant, R_{SH} is the shunt resistance and R_s is the series resistance. The open circuit voltage can be computed as shown in Equation (3):

$$V_{oc} = V + I.R_s \tag{3}$$

The generated current by a PV solar cell relies on how much sunlight it absorbs, the internal resistance of the cell, and the external voltage. Figure 2 depicts the current I vs voltage V output curve of a photovoltaic (PV) cell as a function of illumination intensity. Changes in the cell's current and voltage as a function of light intensity are shown here.

In most cases, the I-V curve may be broken down into two distinct areas: the linear zone and the saturation region. There is a linear area where the current is proportional to the voltage, and the slope of the curve is set by the series resistance of the cell R_s. The term "ohmic region" is often used to describe this area. Increasing the light intensity brings the curve closer to the saturation area. It is the shunt resistance of the cell that determines the slope of the current-voltage curve in the saturation area, when the current is no longer proportional to the voltage R_{SH}.

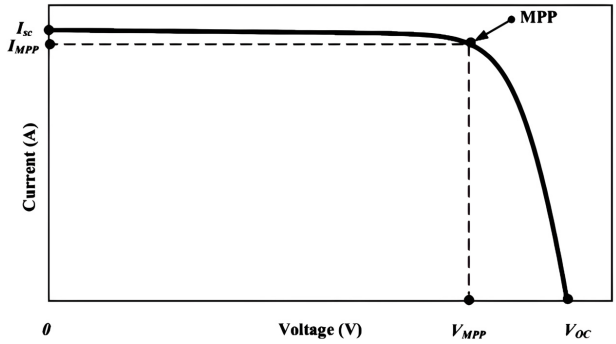

Figure 2. I-V characteristics curves of PV cell [15]

The electrical behavior of a photovoltaic cell (PV cell) under different light and temperature circumstances may be described using the P-V characteristics curves displayed in Figure 3. The P-V characteristics curve's low-light area describes the cell's operating point under very low illumination. Due to the little quantity of current being produced, the cell's voltage is low. Moreover, the cell's power output is often just a few watts in this area.

At the peak of the P-V characteristics curve, when the cell's voltage and power output are both maximal, we get the maximum power point region. The largest amount of power is produced in this area; thus, it's called the "sweet spot" of the curve. When the cell's voltage and current are both at their highest, they are said to be saturating. This is the power-output plateau, when the cell can produce no more power. When the cell's voltage and current are both too high, the P-V characteristics curve enters the overload area. Here, the cell's power production has peaked, and further increases are impossible.

The expression of this maximum power $P_{\max}$ is given by the product of the maximum value of current and voltage as follows:

$$P_{\max} = V_{\max}.I_{\max} \tag{4}$$

The Equation (4) can be described in terms of fill factor FF as shown in Equations (5) and (6):

$$P_{\max} = V_{sc}.I_{sc}.FF \tag{5}$$

$$FF = \frac{P_{\max}}{I_{sc}.V_{sc}} = \frac{I_{\max}.V_{\max}}{I_{sc}.V_{sc}} \tag{6}$$

3.2. PV System Features

Changes in operational conditions, including sun irradiation, moisture levels, and temperature, affect photovoltaic system performance.

The amount of solar irradiation a PV system receives is directly connected to the amount of electricity it produces (Figure 4), and the amount of power produced is inversely proportional to temperature (Figure 5). Changing temperature or solar energy changes the maximum power point. DC-DC converters must be used to alter the array terminal voltage and monitor the maximum power point [17].

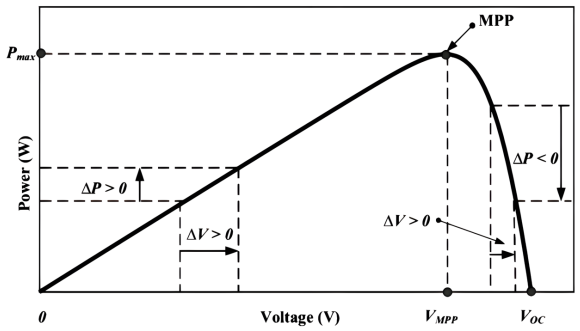

Figure 3. P-V characteristics curves of PV cell [15]

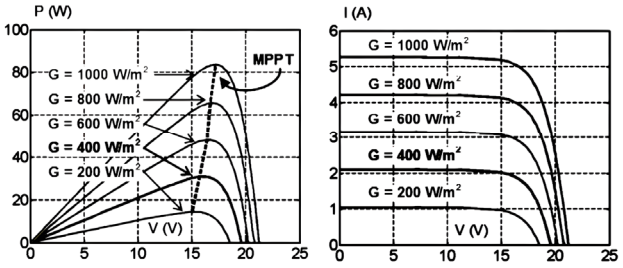

Figure 4. The impact of changes in solar radiation on PV solar cell performance [16]

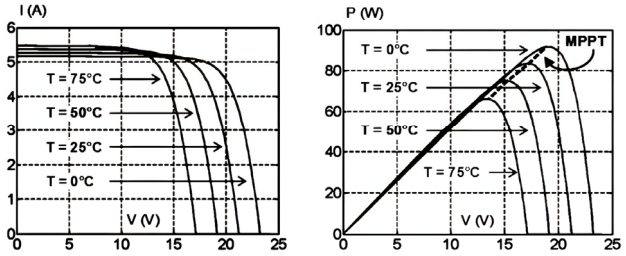

Figure 5. The influence of temperature fluctuations on solar radiation on PV solar cell performance [16]

In case of N_p PV solar modules on parallel, and N_s PV solar modules on series, the current drawn by PV modules can be computed as follows:

$$I_{pv} = N_p.I_{ph} - N_p.I_s.e^{\left(q.V_{pv}+I_{pv}.R_s\right)/Ns.A.K.T} \tag{7}$$

4. MAXIMUM POWER POINT TRACKING MPPT

4.1. DC-DC Converter

Nonlinear PV systems fluctuate in output power due to changing environmental conditions. A DC-DC converter is the best tool for dealing with changes in a PV source's voltage and current. The converter changes the direct current output value from the direct current input voltage. [18] (Figure 6).

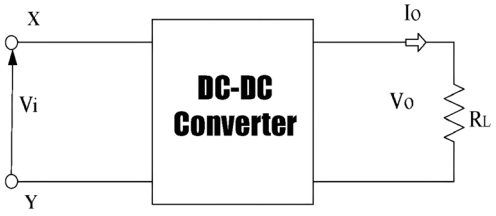

Figure 6. DC-DC converter structure [17]

This adjustment must be done with low converter losses; thus, the transistor will act as a switch and apply the control signal $d(t)$. Figure 7 shows that the control is permitted to remain high for t_{on} and t_{off}.

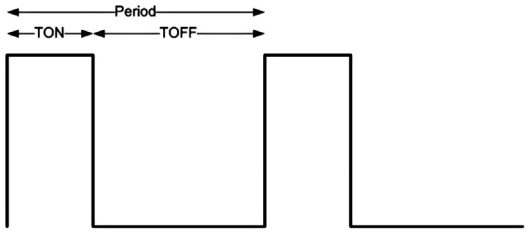

Figure 7. Transistor control signal

The on-device voltage drop reduces the transistor's power loss. Turning off the transistor reduces both the current and electricity wasted. Changing the pulse width while keeping T_s constant changes the average output voltage. With $d(t)= t_{on} /T_s$, the duty cycle is a value from the real interval [0, 1]. Duty cycle equals pulse width/switching time. Resistors are not utilized in DC-DC converters to decrease loss. Inductors and capacitors are used since they don't produce losses under ideal circumstances. Electrical components may be linked and integrated in a number of topologies, each with distinct features. Most transformers are buck-boost, buck, or boost. Buck transformer raises the input voltage, whereas boost converters reduce it. Buck-boost systems produce both voltages [17].

4.2. Buck Converter

The ideal buck converter connects I_g, I_o, V_g, and V_o priested in Equations (8) and (9).

$$V_o = V_g.D \tag{8}$$

$$I_o = I_g.D \tag{9}$$

where, D is the duty cycle in the steady state. By using the law of Ohm's, the converter's R_L load is presented in Equation (10).

$$R' = \frac{R_L}{D^2} \tag{10}$$

To increase the source's work load, adjust 0 to D. For the buck converter, the beginning load must be smaller than the PV module's MPP current in order to draw the most electricity possible.

4.3. Boost Converter

Equations (11) and (12) present the average boost converter output, input, and current values after optimization:

$$V_o = \frac{V_g}{1-D} \tag{11}$$

$$I_o = \frac{I_g}{1-D} \tag{12}$$

The load resistance R' on the input side may be stated as Equation (13). Adjusting D between 0 and 1 reduces the source's load.

$$R' = R(1-D)^2 \tag{13}$$

4.4. Buck Boost Converter

Optimized buck-boost converter output, input, and current averages are described in Equations (14) and (15) [18].

$$V_o = \frac{D}{1-D} V_g \tag{14}$$

$$I_o = \frac{D}{1-D} I_g \tag{15}$$

The analogous expression for R' is present in Equation (16):

$$R' = R\left(\frac{1-D}{D}\right)^2 \tag{16}$$

By altering D, the source's apparent load may be boosted or lessened. The buck-boost converter may work in Zone I or II. According to the study, the optimized buck-boost converter is superior to the other two. Figure 8 shows the buck-boost converter circuit.

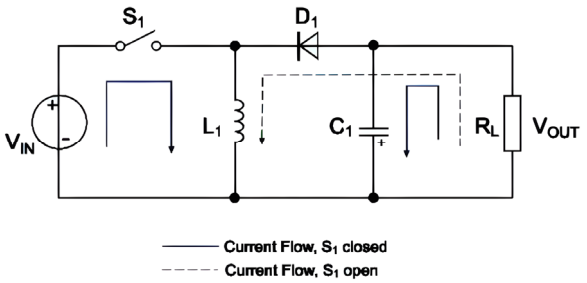

Figure 8. A circuit for buck-boost conversion [19]

To increase the source's workload, adjust 0 to D_1. For the buck converter, the beginning load must be smaller than the MPP current of PV module in order to draw the most electricity possible.

4.5. Fuzzy Logic Outlines

The inputs of an expert are combined with desired outputs using fuzzy logic. In reality, fuzzy logic's applicability is dictated by its four components. Figure 9 shows the overall design of the fuzzy logic system.

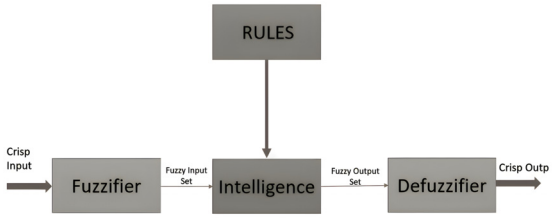

Figure 9. Fuzzy logical system structure [20]

1. Rule-based systems use if-then. Fuzzy logic is used to quantify expert opinion on optimum control.
2. An inference technique that replicates how experts make judgments by first "comprehending" information and then utilizing that knowledge to regulate input components.
3. Inputs are processed using a fuzzy logic interface to give information for rule formulation and application.
4. A direct de-compilation interface "feeds" the algorithm results of inference.

4.5.1 Fuzzy Logic Membership Functions

This procedure values inputs that may be functional overlaps. The membership function affects the final outcome. Configuration, or "form," is an important membership function-defining component. Figure 10 shows membership functions, definitions, and graphs.

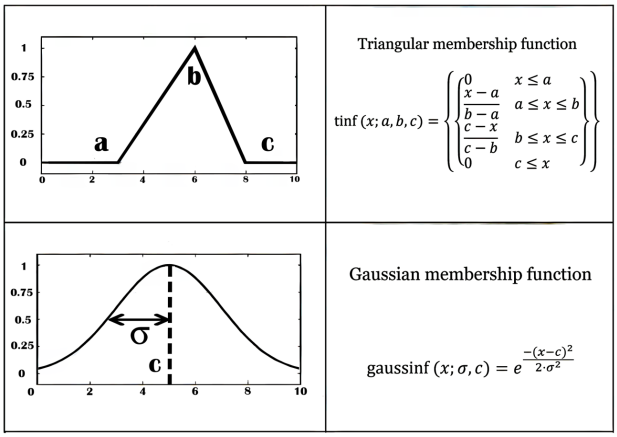

Figure 10. Different types of membership function [19]

4.5.2 Fuzzy Logic Defuzzification

This refines confusing inference engine findings (crisp). Determining which defuzzification approach is suitable for a given application is more art than science (Figure 11). The Centroid of Gravity (COG) approach has supplanted prior methods due to its simplicity.

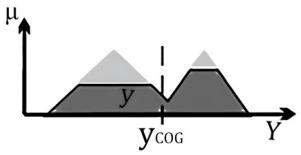

Figure 11. Defuzzification method of Center of Gravity method (COG)

In Figure 11, the centroid of gravity (COG) can be computed as follows:

$$y_{COG} = \frac{\int_{y \in Y} y \mu_y(y)\, dy}{\int_{y \in Y} \mu_y(y)\, dy} \tag{17}$$

5. SIMULATION RESULTS

Figure 12 provides a high-level overview of the whole MPPT solar PV controller model created in the MATLAB/Simulink environment. It is made up of a battery, a micro grid, an MPPT charge control block, a DC-DC regulator, and a PV solar array.

5.1. MPPT and PI Controller Implementation

Figure 13 shows the MPPT and PI Controller implementation and the differential change in power and voltage block diagram and the error generating block diagram are presented in Figure 12.

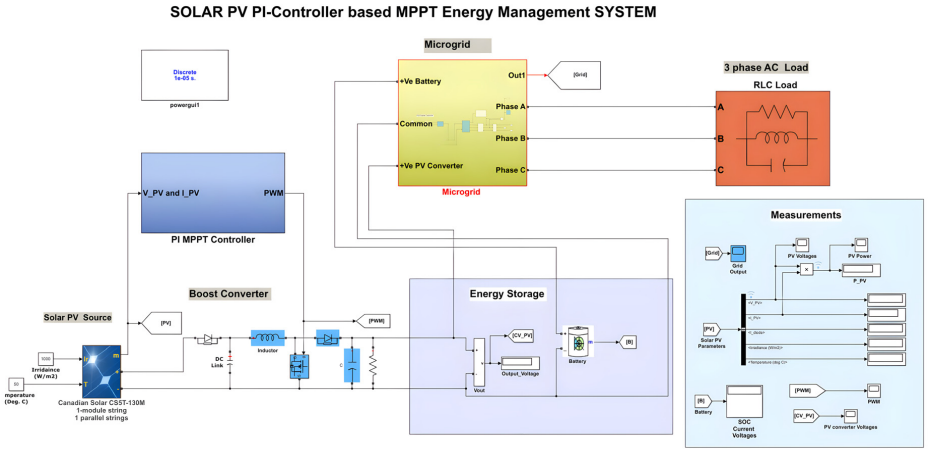

Figure 12. complete Simulink model design SOLAR PV based on MPPT

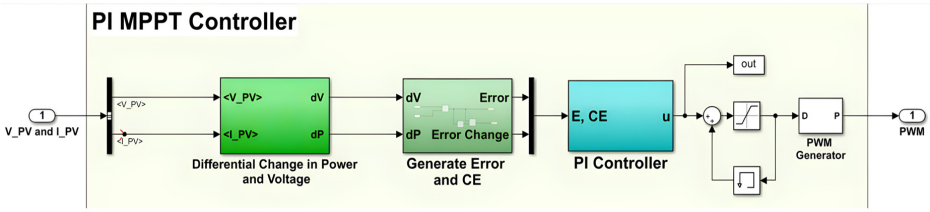

Figure 13. PI controller implementation

The response indicates the output's waveform of the solar PV solar system with maximum power delivered by PV system through MPPT with PI technique is illustrated in Figure 14. The grid output voltages are shown in Figure 15, the waveform is sinusoidal waveform but not pure.

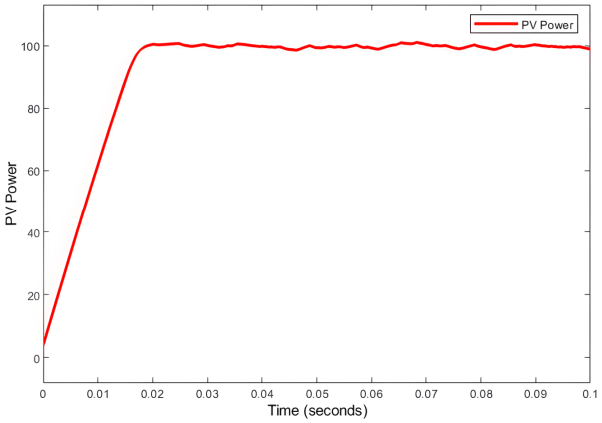

Figure 14. PV power with PI controller

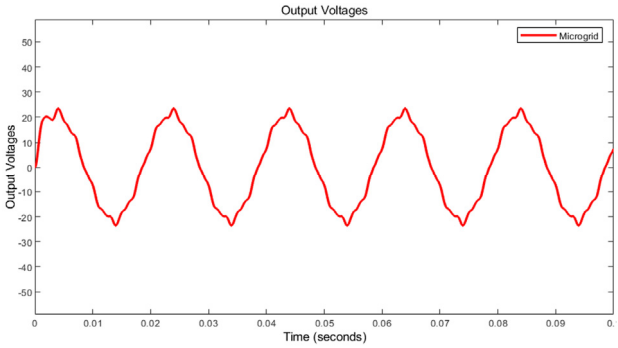

Figure 15. Grid output voltages

The PV converter PWM signal is shown by constant duty cycle interval in Figure 16. The duty cycle of PWM generator is shown as we can achieve the varying duty cycle of system.

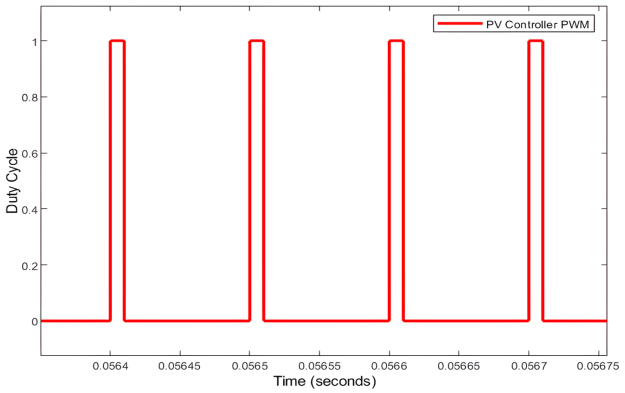

Figure 16. PV converter PWM signal

The output voltages of 25 volts PV converter are achieved with implementation of PI controller is shown in Figure 17. The maximum power achieved with PI controller MPPT is 99.02 Watts.

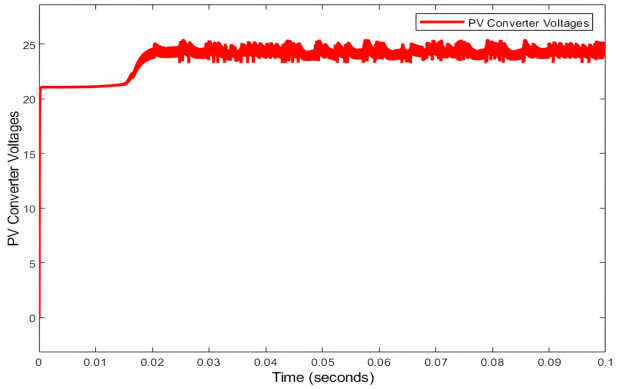

Figure 17. PV converter voltages with PI controlled MPPT

5.2. MPPT and FLC Controller Implementation

The FLC based MPPT is employed for increasing the PV module voltage (Figure 18). The recommended approach employs FLC to start the control commands to the output buck boost converter when changes in the current and voltage across the PV panel occur.

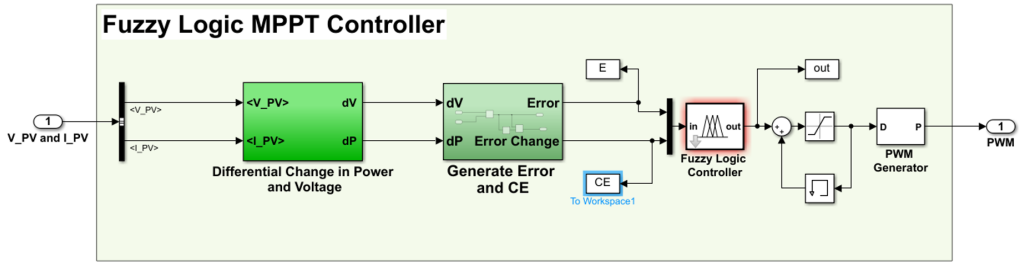

Figure 18. Fuzzy logic controller system block diagram

It is noticeable that the simulation of Fuzzy system delivers the battery output voltages of 23 V at state of charge of 50, and power of PV is almost 106 Watts, the voltages supplied by PV system is 22 v and current drawing through PV system is 4.7 amp, in case of solar radiation of 1000 W/m2 with a solar temperature of 50 °C. Figure 19 shows the solar PV system's output waveform with the highest power supplied by the PV system utilizing MPPT with Fuzzy method.

The PV converter PWM signal is shown in Figure 20 by constant duty cycle interval. The duty cycle of PWM generator is presented as we can achieve the varying duty cycle of system. The output voltages of 25V PV converter are achieved with implementation of FLC controller is shown in Figure 20. Fuzzy controller MPPT can provide a maximum power of 106.1 watts.

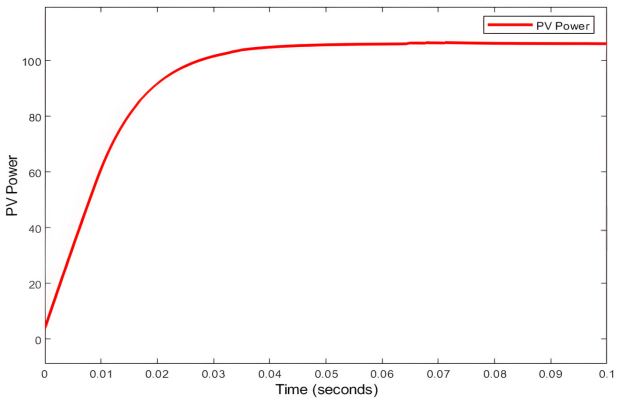

Figure 19. PV power with fuzzy control

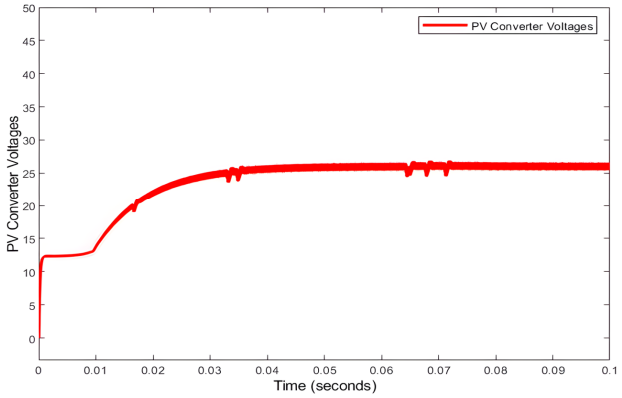

Figure 20. Converter voltages

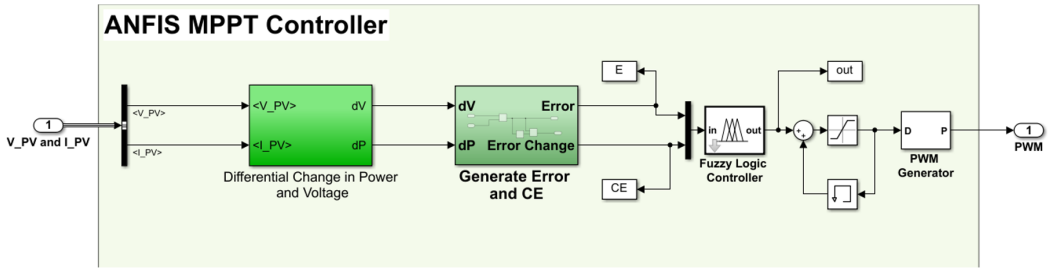

Figure 21. ANFIS controller system block diagram

5.3. MPPT and ANFIS Controller Implementation

This is a proposal for an ANFIS logic-based MPPT controller to expand the PV module (Figure 15). When changes in the current and voltage across the PV panel occur, the suggested technique uses the ANFIS based (FLC) to begin the control commands to the output buck boost converter.

It is observed that the simulation of ANFIS system delivers the battery output voltages of 23.8 V at state of charge of 50, and power of PV is almost 111 Watts, the voltages supplied by PV system is 23 v and current drawing through PV system is 4.6 amp, at applied solar irradiance of 1000 W/m^2 with solar heat temperature of 50 degree centigrade. The response indicates the output waveform of the solar PV system with maximum power delivered by PV system through MPPT with ANFIS technique is shown in Figure 22.

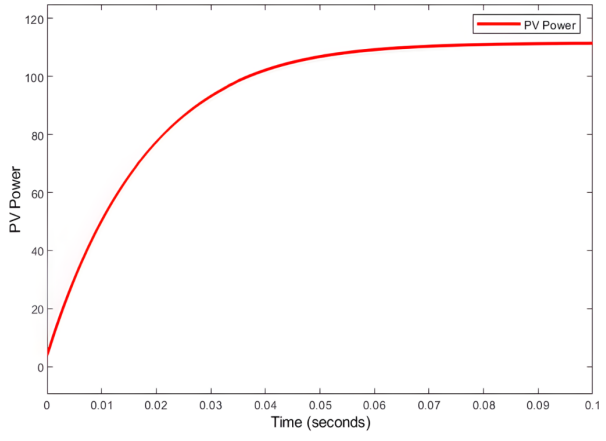

Figure 22. Maximum power achieved with ANFIS

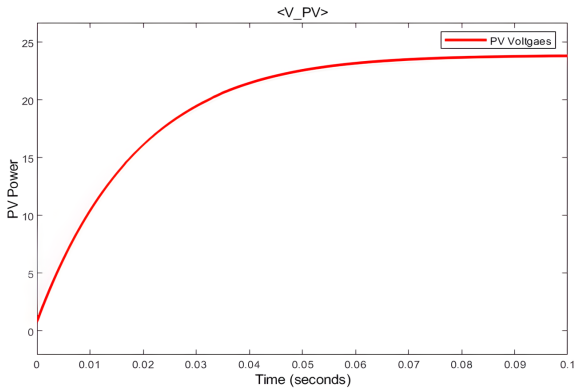

Figure 23. PV controller voltages with ANFIS controlled MPPT

The PV controller Voltages with MPPT based ANFIS response indicates the output waveform of the solar PV system with maximum power delivered by PV system through MPPT with ANFIS technique is illustrated in the Figure 23. The output voltages of 28V PV converter are achieved with implementation of ANFIS controller.

6. CONCLUSIONS

Our research-based effort ensures that the examination of various MPPT methods and approaches is done while accounting for various sun irradiation effects. We have compared many potent technology-based methods for implementing MPPT control and obtaining regulated output with better outcomes. To maintain MPPT of the PV solar array with effective and better output responsiveness, we have built one of the MPPT control methods. For optimal power-point-tracking, we made sure the controller was set up with a Boost transducer and a solar array-optimized MPPT.

For improved, reliable, and efficient output outcomes, a robust DC-DC boost regulator will be created and simulated to build the best solar array MPPT controller. The Fuzzy Controller MPPT Controller can provide a maximum power of 106.1 W. The ANFIS MPPT adaptive fuzzy neural inference system is used to maximize the harvested energy of the PV solar array model. MPPT is completed with the ANFIS MPPT control application, which results in an output response with few oscillations and undesirable noise, as well as the removal of undesirable output factors.

NOMENCLATURES

1. Acronyms

MPPT	Maximum Power Point Tracking
PI	Proportional-Integral
ANFIS	Adaptive Neuro Fuzzy Inference System
PV	Photovoltaic
P&O	Perturbation and Observation
CV	Constant Voltage
INC	Increment Conduction
FLC	Fuzzy Logic Controller
ANN	Artificial Neural Networks
VF/CF	Voltage/Current Feedback
IDCOL	Infrastructure Development Company Limited
COG	Centroid of Gravity
TSC	Technical Standard Committee
TSC	Technical Standard Committee

2. Symbols / Parameters

I_{ph}: The produced current
q: The charge of electron
K: The Boltzmann's constant
R_{SH}: The shunt-resistance
R_s: The series-resistance
V_{oc}: The open-circuit-voltage
P_{max}: The power at maximum
V_{max}: The voltage at maximum
I_{max}: The current at maximum
FF: The fill factors
N_p: The quantity of PV solar modules on parallel
N_S: The quantity of PV solar modules on series
D: The duty cycles
R: The converter's dc resistance load

REFERENCES

[1] N.M. Tabatabaei, S. Mortezaei, A. Abbasi, S. Gorji, "Maximum Power Point Tracking of Ongrid Photovoltaic Systems by Providing a Fuzzy Intelligent-PSO Method Based on a Controllable Inverter with Adaptive Hysteresis Band", International Journal on Technical and Physical Problems of Engineering (IJTPE), Issue 37, Vol. 10, No. 4, pp. 15-24, December 2018.

[2] T.A. Ocran, J. Cao, B. Cao, and X. Sun, "Artificial Neural Network Maximum Power Point Tracker for Solar Electric Vehicle", Tsinghua Science and Technology, Vol. 10, No. 2, pp. 204-208, April 2005.

[3] Aneka Listrik, "PLCs and Fuzzy Logic", Aneka Listrik, 2008, https://anekalistrik.wordpress.com/2008/12/page/2/, February 2023.

[4] D. Spiers, J. Royer, "Guidelines for the Use of Batteries in Photovoltaic Systems", Finland: Varennes Espoo: CANMET Energy Diversification Research Laboratory (CEDRL): Neste Advanced Power System (NAPS), pp. 1-344, 1998.

[5] W. Press, "Advanced Applications of Electrical Engineering", The 7th WSEAS International Conference on Application of Electrical Engineering (AEE'08), pp. 1-534, 2008.

[6] M. Venkateshkumar, "Fuzzy Controller-Based MPPT of PV Power System", Fuzzy Logic Based in Optimization Methods and Control Systems and Its Applications, pp. 1-10, October 2018.

[7] J. Bilbao, E. Bravo, O. Garcia, C. Varela, C. Rebollar, "Load Optimization Methods for a Maximum Power Point Tracker used in Solar Panels", International Journal on Technical and Physical Problems of Engineering (IJTPE), Issue 37, Vol. 10, No. 4, pp. 48-53, December 2018.

[8] W. Wu, N. Pongratananukul, W. Qiu, K. Rustom, T. Kasparis, I. Batarseh, "DSP-Based Multiple Peak Power Tracking for Expandable Power System", Eighteenth Annual IEEE Applied Power Electronics Conference and Exposition, APEC '03, pp. 1-6, 2003.

[9] H. Attia, "High Performance PV System Based on Artificial Neural Network MPPT with PI Controller for Direct Current Water Pump Applications", International Journal of Power Electronics and Drive Systems (IJPEDS), Vol. 10, No. 3, p. 1329, September 2019.

[10] A. Faizal, Sutoyo, Mulyono, R. Yendra, A. Fudholi, "Design Maximum Power Point Tracking (MPPT) on Photovoltaic Panels using Fuzzy Logic Method", American Journal of Engineering and Applied Sciences, Vol. 9, No. 4, pp. 789-797, April 2016.

[11] M.D. Rokonuzzaman, M. Hossam-E-Haider, "Design and Implementation of Maximum Power Point Tracking Solar Charge Controller", The 3rd International Conference on Electrical Engineering and Information Communication Technology (ICEEICT 2016), pp. 1-5, September 2016.

[12] D.S. Karanjkar, S. Chatterji, A. Kumar, S.L. Shimi, "Fuzzy Adaptive Proportional-Integral-Derivative Controller with Dynamic Set-Point Adjustment for Maximum Power Point Tracking in Solar Photovoltaic System", Systems Science and Control Engineering, Vol. 2, No. 1, pp. 562-582, October 2014.

[13] S. Assahout, H. Elaissaoui, A. El Ougli, B. Tidhaf, H. Zrouri, "A Neural Network and Fuzzy Logic based MPPT Algorithm for Photovoltaic Pumping System", International Journal of Power Electronics and Drive Systems (IJPEDS), Vol. 9, No. 4, p. 1823, December 2018.

[14] A. Ulinuha and A. Zulfikri, "Enhancement of Solar Photovoltaic Using Maximum Power Point Tracking

Based on Hill Climbing Optimization Algorithm", Journal of Physics: Conference Series, Vol. 1517, pp. 1-7, April 2020.
[15] S. Hamadi, M. Rezaoui, K. Milod, "Comparison of Fuzzy Logic and P&O MPPT Techniques for Solar Photovoltaic System", The 2nd International Workshop on Signal Processing Applied to Rotating Machinery Diagnostics, pp. 1-11, April 2018.
[16] I. Hamdan, A. Maghraby, O. Noureldeen, "Stability Improvement and Control of grid-connected Photovoltaic System during Faults Using Supercapacitor", SN Applied Sciences, Vol. 1, No. 12, pp. 1-19, November 2019.
[17] W. Robert, Erickson, "Fundamentals of Power Electronics", Springer Science and Business Media, p. 733, 2013.
[18] X. Guo, J. Chen, and Q. Liu, "Real-Time and Grid-Connected Control of PV Power System", The 2011 International Conference on Advanced Power System Automation and Protection, pp. 923-228, October 2011.
[19] H. Kumar, R.K. Tripathi, "Simulation of Variable Incremental Conductance Method with Direct Control Method Using Boost Converter", The 2012 Students Conference on Engineering and Systems, pp. 1-5, March 2012.
[20] N. Mohan, T.M. Undeland, W.P. Robbins, "Power Electronics: Converters, Applications, and Design", Wiley India, p. 811, New Delhi, India, 2007.

BIOGRAPHIES

Name: **Sarmad**
Middle Name: **Khalid Waheeb**
Surname: **Aldoori**
Birthday: 08.08.1989
Birth Place: Tikrit, Iraq
Bachelor: Electrical Engineering, Electrical, Tikrit University, Tikrit, Iraq, 2015
Master: Electrical and Electronics Engineering, Faculty, University of Cankiri, Cankiri, Turkey, 2023

Name: **Mahmud Esad**
Surname: **Yigit**
Birthday: 14.06.1989
Birth Place: Cankiri, Turkey
Bachelor: Electronics and Communication Engineering, Faculty of Electrical and Electronics Engineering, Istanbul, Turkey, 2011
Master: Telecommunication Engineering, Graduate School, Istanbul Technical University, Istanbul, Turkey, 2014
Doctorate: Student, Telecommunication Engineering, Graduate School, Istanbul Technical University, Istanbul, Turkey, Since 2014
The Last Scientific Position: Research Assistant, Faculty of Engineering, Cankiri Karatekin University, Cankiri, Turkey, Since 2020
Research Interests: Electromagnetics, Microwave Systems, Antennas, Optimization, Communications.
Scientific Publications: 16 Papers, 1 Thesis
Scientific Memberships: IEEE Student Member

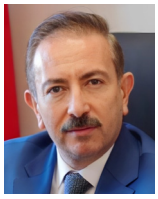

Name: **Murat**
Surname: **Ari**
Birthday: 22.05.1969
Birth Place: Cankiri, Turkey
Bachelor: Electrical and Electronics Engineering, Faculty of Engineering of Gaziantep, Middle East Technical University, Ankara, Turkey, 1992
Master: Electrical and Electronics Engineering, Institute of Science, Gazi University, Ankara, Turkey, 1999
Doctorate: Electronic Computer Education, Institute of Science, Gazi University, Ankara, Turkey, 2004
The Last Scientific Position: Prof., Faculty of Engineering, Cankiri Karatekin University, Cankiri, Turkey, Since 2017
Research Interests: Electrics, Electronics, Embedded Systems, Communications, Optoelectronics
Scientific Publications: 76 Papers, 1 Patent, 5 Projects, 3 Theses
Scientific Memberships: IJTPE Journal Scientific Board, Sub Area Editor of Gazi Journal of Science, 5 National Academic Memberships